

¹Yibo Liu □²Yirui Wang³Qianfei Xu⁴Yuxuan He¹Supeng Wu

Optimal Dispatch of Electric-Hydrogen-Transport Coupling for Offshore Island Based on Improved Dung Beetle Optimizer



Abstract: - There are abundant renewable energies in the region of offshore islands, and the progress of electrolytic hydrogen production and hydrogen storage technology has promoted the local consumption of distributed energy. This paper proposes a low carbon economic dispatching method for offshore islands, which takes into account self-sufficiency and shared hydrogen storage (SHS). Firstly, a bidirectional coupling framework of hydrogen fuel cell ship (HFCS) transportation network and island new energy system is designed. With the optimization objectives of reducing the operation cost of transportation network and ocean islands, improving the energy self-consistency rate and reducing the carbon emission cost, this paper comprehensively considers the operation constraints of new energy, marine transportation network, hydrogen energy Storage system and Short-term Hydrogen Storage on ocean islands. The coupling optimization dispatching model of low-carbon economy for offshore islands with STHS and SHS is established. On this basis, Improved Dung Beetle Algorithm (IDBO) is used to balance local optimization and global optimization capabilities by using the dung beetle action mutation strategy and reverse learning strategy based on population similarity. Finally, an improved IEEE 6-node system diagram is given to verify the feasibility of method for improving the self-consistency rate of new energy sources and reducing the cost of carbon emissions in offshore islands, and the effectiveness of the improved algorithm.

Keywords: pelagic islands; electric-hydrogen-transport coupling; hydrogen storage; coordinated optimization

1. Introduction

As an important platform for the development of marine resources, ocean-going islands cannot be fully developed because they are located in the far sea and are limited by resource replenishment. If the green energy sources such as wind and light can be effectively utilized, it will break through the resource limitation bottleneck of the existing ocean-going islands that rely solely on diesel engines for power generation[1]. If the offshore island group is taken as a whole and a self-consistent energy system of source-load-storage-charging is constructed, the self-sustaining resources of the group will be realized [2-3].

Nowadays, the research on offshore island power supply system is relatively mature. The distributed micro grid on the island is mainly interconnected with the mainland main power grid through DC transmission lines. Literature [4] develops a search algorithm that takes into account the combined search area for the transmission optimization of offshore wind power and the optimal configuration of radial transmission systems. Literature [5] develops a new configuration of hybrid offshore storm energy system, which can provide stable power to remote islands or coastal communities. Literature [6] innovates the island's energy use mode: renewable energy is exerted seasonally, and submarine cables are used to stabilize and isolate the power grid system. However, because the offshore islands are close to the mainland, there is no need to consider transportation problems, so there are many technical limitations and problems in applying the accumulated experience of previous research to offshore islands.

¹ College of Electrical Engineering and New Energy, China Three Gorges University, 443002, China. Email:liuyibo1_1@163.com

²The School of international education, North China Electric Power University, Beijing, 102206, China

³The School of Electrical and Electronic Engineering, North China Electric Power University, Beijing, 102206, China

⁴College of Computer, Hubei University of Education, 443000, China

Therefore, the concept of integrated energy supply system for ocean-going islands group has been proposed[7]. In [8], an island self-consistent energy system is constructed in this paper. In this system, the integration of two independent systems, island energy supply and maritime traffic, can not only make full use of green resources and maximize the self-consistency rate of energy, but also effectively use the distributed energy and energy storage systems in the island group to realize high-level local consumption of energy. In [9], there is a main island, which is both a resource-rich island and a load center island. The island's diesel generators, fans and photostatic supply power to the island's main electrical loads. If there is surplus between wind power generation and photovoltaic power generation, the surplus energy can be stored in the hydrogen storage tank through chemical reaction. In [10], a low-carbon hybrid energy system consisting of energy storage batteries, photovoltaic systems and gas/diesel engines is constructed. In[11], taking Bensa Island of Italy as the research object, deep learning method is used to dispatch renewable energy, which shows that the consumption of fossil fuels can be reduced and the economy of system operation can be improved. In [12], a multi-time scale rolling coordination scheduling method is proposed for island microgrids with high proportion of tidal flow energy access and demand response resources. In [13], the joint random scheduling of island grid energy and standby generation provided by diesel and gas generators, photovoltaic and battery energy storage systems (BESS) is studied. In the current research on energy dispatch of offshore island groups, energy transfer is mostly carried out by electric storage ships. Hydrogen fuel cell ships have the advantages of environmental protection, short refueling time and long cruising distance, but there are few studies on hydrogen energy as the power source of new energy storage transportation equipment.

For ocean-going islands, the existing research is mainly based on the inter-island discrete energy transmission mode of power exchange ships, and the clean electric energy produced by resource-rich islands is transported to other islands in the form of mobile battery packs to supply loads, so as to realize the optimal economic operation of electric energy. Literature [14] divides ocean islands into resource-rich islands and load center islands, and proposes a new energy management system based on battery logistics of electric ships, which optimizes the operation of middle and upper isolated micro grid clusters. Literature [15] puts forward a scene-based stochastic optimal dispatching model, and analyzes the comprehensive influence of environmental factors such as wind, solar radiation and ocean current on the transportation of electric boats in detail, so as to carry out effective energy management. Literature [16] replaces part of the cable network with all-electric ship routing, and proposes an energy transmission route using electric ships to transport battery energy between islands, which reduces the comprehensive operating cost by transporting renewable energy. Literature [17] puts forward an energy coordination and optimization strategy based on shared power exchange ship, which can effectively improve the renewable energy consumption rate and operation economy of cluster islands. Literature [18] takes into account traffic network constraints and models the discrete energy flow of a mobile energy storage system. By adjusting the spatiotemporal distribution of the mobile energy storage system, the power flow distribution of the system is optimized to reduce network losses. Literature [19] proposed a discrete energy transfer model for mobile energy storage systems based on a spatiotemporal network model, and analyzed the impact of mobile energy storage systems on the economic and reliability of power grid operation. Literature [20] proposed a discrete energy emergency power supply strategy based on mobile energy storage stations for islanded operation

mode under fault conditions, and evaluates the reliability of distribution network operation using Markov chains. However, the current research only focuses on the strategies of island energy consumption, the concept of shared hydrogen storage has not been introduced in the existing research on integrated energy supply of clustering island groups.

With the development of hydrogen fuel cell and hydrogen energy storage technology, hydrogen fuel cell ships that can be used will transport hydrogen energy to the main hydrogenation stations and substations on the islands for use on other islands. If the main load on the island cannot be met, the hydrogen energy in the island group will be sent to the island to supply the main load on the island. Therefore, coupling the island with the transportation network through a new type of hydrogen energy storage is an important measure to realize energy self-built island group.

The major contributions of this paper are described below:

- Considering the operation constraints of new energy, maritime traffic network and hydrogen energy storage system in ocean islands and short-term hydrogen energy storage and shared hydrogen energy storage services, the load center island and maritime traffic network are finely modeled.
- A two-level optimal dispatching model of ocean island coupled with electricity, hydrogen and transportation is established, and a solution method based on improved dung beetle optimization algorithm is given.
- The feasibility and effectiveness of the proposed method are verified by an example simulation, and provide useful reference for the low-carbon economic operation of offshore islands and maritime transportation networks under the background of energy transformation.

2. Ocean Island Energy System-Maritime Traffic Network Bidirectional Coupling Architecture

The two-way coupling architecture of ocean island energy system and maritime traffic network includes power network and maritime traffic network dominated by HFCS, as shown in Figure 1. Ocean-going island energy system is responsible for the access of distributed new energy, power supply of electric load, interface of diesel generator and power supply of hydrogen production equipment by electrolysis of water. The distributed new energy firstly supplies power to the island load, and the residual electricity can be converted into hydrogen energy for HFCS or hydrogen energy storage system. Hydrogenation main station and substation of marine transportation network provide energy for HFCS, and STHS and SHS can make up for the shortage of hydrogen energy. On the other hand, the hydrogen energy storage system can also supply power to the electric load during the peak period. The two-way coupling architecture of ocean island energy system and maritime transportation network makes the two separated systems of energy and transportation integrate with each other and develop together, and finally forms a clean, low-carbon, integrated and efficient energy Internet.

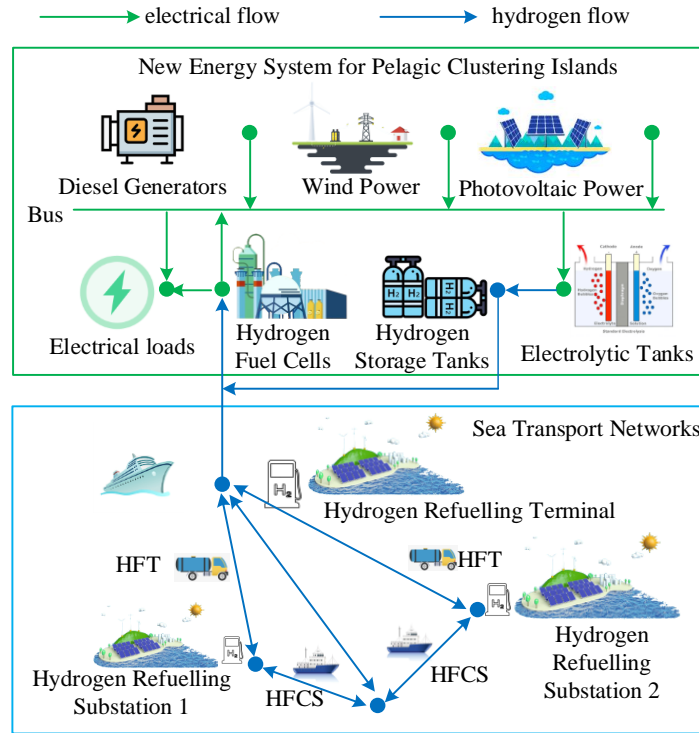


Figure 1. Two-way coupling architecture of island energy system and maritime traffic network

3. electricity-hydrogen-traffic coupling model

3.1. Load Center Island Model

The load center island is equipped with an integrated power supply system of active power, network power and load. In the process of operation, the constraints such as power flow constraint, line transmission power constraint, voltage over-limit, diesel generator output constraint and distributed energy output constraint need to be considered.

1) Power flow constraint:

$$\begin{cases} \sum_{j \in i} P_{DG} + P_G^i + P_{d\Sigma}^i - U_i \sum_{j \in i} U_j (G_{ij} \cos \theta_{ij} + B_{ij} \sin \theta_{ij}) = P_D^i \\ \sum_{j \in i} Q_{DG} + Q_G^i + Q_{d\Sigma}^i - U_i \sum_{j \in i} U_j (G_{ij} \sin \theta_{ij} - B_{ij} \cos \theta_{ij}) = Q_D^i \end{cases} \quad (1)$$

Where: $j \in i$ means that the source, storage and payload are properly connected to node i ; U_i is the voltage amplitude of node i ; θ_{ij} is the power angle between nodes i and j ; $G_{ij} + B_{ij}$ is the admittance parameter;

P_{DG} 、 P_G^i 、 $P_{d\Sigma}^i$ 、 P_D^i 、 Q_{DG} 、 Q_G^i 、 $Q_{d\Sigma}^i$ 、 Q_D^i are respectively distributed new energy, diesel generator, energy storage and active power and reactive power of load.

2) Line power constraint:

$$-P_{l,\max} \leq U_i U_j (G_{ij} \cos \theta_{ij} + B_{ij} \sin \theta_{ij}) \leq P_{l,\max} \quad (2)$$

Where: $-P_{l,\max}$ is the maximum transmission power (nodes i and j at both ends).

3) Voltage constraint:

$$U_{\min} \leq U_i \leq U_{\max} \quad (3)$$

Here: U_{\min} 、 U_{\max} are the upper and lower bounds of the node voltage amplitude respectively, where 1.1 and 0.9 are taken.

4) Output constraint of diesel generator:

$$P_{G\min}^i \leq P_G^i \leq P_{G\max}^i \quad (4)$$

Where: $P_{G\max}^i$ is the maximum output of the diesel generator, generally taking the indicated output. $P_{G\min}^i$ is the minimum output, taking 0.3 P_{GN}^i .

5) Wind-solar distributed energy output constraint

$$\begin{cases} P_{\min}^{WT} \leq P_{WT}(t) \leq P_{\max}^{WT} \\ P_{\min}^{PV} \leq P_{PV}(t) \leq P_{\max}^{PV} \end{cases} \quad (5)$$

Where: P_{\min}^{WT} 、 P_{\min}^{PV} are the minimum output of wind-solar distributed energy and P_{\max}^{WT} 、 P_{\max}^{PV} are the maximum output of wind-solar distributed energy respectively.

6) Hydrogen production model of wind-solar distributed energy surplus electricity:

$$\begin{cases} P_{ex}(t) = P_{pv}(t) + P_{wind}(t) - P_{e-load}(t) \\ P_{eP2G}(t) = \eta_{p2G} P_{ex}(t) \\ P_{eP2G}(t) + E_{H_2}(t-1) \leq E_{H_2}^{\max} \end{cases} \quad (6)$$

Where: $P_{ex}(t)$ refers to the residual power of wind-solar distributed energy in t period; $P_{eP2G}(t)$ refers to the electric power used by electrolytic hydrogen module in t period; $P_{pv}(t)$ 、 $P_{wind}(t)$ are the output of wind-solar distributed energy in t period; $P_{e-load}(t)$ refers to the electric load in t period; η_{p2G} refers to the energy conversion efficiency; $E_{H_2}(t)$ is the storage capacity of hydrogen in t period and $E_{H_2}^{\max}$ is upper limit of capacity of hydrogen storage equipment.

7) Construction of hydrogen energy storage model:

Energy storage of hydrogen consists by hydrogen storage tank, hydrogen production device and hydrogen fuel cell. The tank stores hydrogen, the electrolytic hydrogen production device consumes electric energy to make hydrogen, and the cell provides electric energy by burning hydrogen. The calculation process of energy stored in tank is shown as follows:

$$E_{H_2}(t) = E_{H_2}(t-1) + \eta_{p2G} P_{eP2G}(t) \Delta t - \frac{P_{FC}(t)}{\eta_{FC}} \Delta t \quad (7)$$

The variable t represents sequence number of the scheduling period. $E_{H_2}(t)$ represents the energy in the energy storage in the t scheduling period; η_{p2G} and η_{FC} are respectively the energy conversion efficiency of the hydrogen production device and the cell; Δt represents the time span of the scheduling period.

Life decay cost corresponding to hydrogen energy storage power fluctuation;

$$C_{\lambda_FL} = \sum_{t=2}^T \kappa_{\lambda_FL} |P_{\lambda_t} - P_{\lambda_t-1}| r_{\lambda_t} r_{\lambda_t-1}, \forall \lambda \in \{ED, FC\} \quad (8)$$

Where, K_{λ_FL} represents the life decay cost corresponding to the unit fluctuating power of the device and fuel cell; P_{λ_t} represents the electric power of hydrogen production device and hydrogen fuel cell; r_{λ_t} indicates the start-stop state of device and fuel cell.

The start-stop costs of hydrogen production device and fuel cell are shown in the formula:

$$C_{\lambda_SU} = \sum_{t=1}^T \kappa_{\lambda_SU} r_{\lambda_SU_t}, \forall \lambda \in \{ED, FC\} \quad (9)$$

$$C_{\lambda_SD} = \sum_{t=1}^T \kappa_{\lambda_SD} r_{\lambda_SD_t}, \forall \lambda \in \{ED, FC\} \quad (10)$$

Where, K_{λ_SU} and K_{λ_SD} are respectively the unit start-stop costs of the device and the fuel cell; $r_{\lambda_SU_t}$ and $r_{\lambda_SD_t}$ respectively show the start-stop states of the device and the fuel cell.

Maintenance cost of device and hydrogen fuel cell

$$C_{\lambda_OM} = \sum_{t=1}^T \kappa_{\lambda_OM} \Delta t, \forall \lambda \in \{ED, FC\} \quad (11)$$

Where, K_{λ_OM} represents the maintenance cost per unit time of the hydrogen production device and the fuel cell.

The life decay cost corresponding to the historical operation time of the device and the fuel cell is shown in the formula:

$$C_{\lambda_AGE} = \sum_{t=1}^T \kappa_{\lambda_AGE} \frac{\Delta t}{T_{\lambda_LT}}, \forall \lambda \in \{ED, FC\} \quad (12)$$

Where, K_{λ_AGE} refers to the life decay cost corresponding to the unit operation time of device/fuel cell; T_{λ_LT} indicates the expected life of device/hydrogen fuel cell.

The total operating cost of hydrogen energy storage is:

$$C_{HS} = C_{\lambda_FL} + C_{\lambda_SU} + C_{\lambda_SD} + C_{\lambda_OM} + C_{\lambda_AGE}, \forall \lambda \in \{ED, FC\} \quad (13)$$

3.2. Maritime traffic network model

The hydrogen load of HFCS is mainly affected by mileage, return time and supply and demand of hydrogen refueling stations. The traffic network model is established as follows.

The probability density function of the last return time of the daily user is:

$$f_i(x_i) = \begin{cases} \frac{1}{\gamma_i \sqrt{2\pi}} \exp\left[-\frac{(x_i - \psi_i)^2}{2\gamma_i^2}\right], \psi_i - 12 < x_i \leq 24 \\ \frac{1}{\gamma_i \sqrt{2\pi}} \exp\left[-\frac{(x_i + 24 - \psi_i)^2}{2\gamma_i^2}\right], 0 < x_i \leq \psi_i - 12 \end{cases} \quad (14)$$

Where: x_i is the last return time of the user, ψ_i is the expected value and γ_i is the standard deviation.

The probability density function of mileage traveled by HFCS users is defined as:

$$f_s(x_s) = \frac{1}{\gamma_s x_s \sqrt{2\pi}} \exp\left[-\frac{(\ln x_s - \psi_s)^2}{2\gamma_s^2}\right] \quad (15)$$

Where: x_s is the last return time of the user, ψ_s is the expected value and γ_s is the standard deviation.

Hydrogenation duration of HFCS is:

$$T_s = \frac{SE}{P_s \sigma_s} \quad (16)$$

Where: T_s is hydrogenation duration; S refers to daily mileage; P_s is hydrogenation quantity; σ_s is hydrogenation efficiency; E refers to hydrogen consumption per unit kilometer.

Single-station hydrogenation demand

$$N_{m,HFCS} \leq N_{m,H} \quad (17)$$

Where: $N_{m,HFCS}$ refers to the number of existing HFCS in the M-Th hydrogen refueling station and $N_{m,H}$ refers to the number of HFCS acceptable in the M-Th hydrogen refueling station.

Total hydrogenation demand of transportation network

$$\sum_{m=1}^M M_{m,cqz} \geq \sum_{e \in N_{HFCS}} M_{e,HFCS} \quad (18)$$

Where: M is the number of hydrogen refueling stations in the transportation network, $M_{m,cqz}$ is the capacity of hydrogen storage stations, the e-Th HFCS capacity and N_{HFCS} is the number of HFCS.

Short-term hydrogen storage model

$$\begin{cases} S_{w,t}^{STHS} = (1 - \alpha_{loss}^{STHS}) S_{w,t-1}^{STHS} + (P_{w,t,abs}^{STHS} \eta_{abs}^{STHS} - P_{w,t,rel}^{STHS} \eta_{rel}^{STHS}) \Delta t \\ 0 \leq P_{w,t,abs}^{STHS} \leq C^{STHS} \\ 0 \leq P_{w,t,rel}^{STHS} \leq C^{STHS} \\ 0 \leq S_{w,t}^{STHS} \leq C^{STHS} \end{cases} \quad (19)$$

Where: $P_{w,t,abs}^{STHS}$, $P_{w,t,rel}^{STHS}$ and $S_{w,t}^{STHS}$ are respectively the storage capacity of hydrogen per unit time, the release capacity of hydrogen per unit time and the total amount in short-term hydrogen storage; η_{abs}^{STHS} , η_{rel}^{STHS} and α_{loss}^{STHS} are respectively the storage efficiency of hydrogen, release efficiency of hydrogen and self-release rate of STHS; C^{STHS} is the configured capacity of STHS and Δt is the unit time step.

Shared hydrogen energy storage model

$$\begin{cases} S_{w,t}^{SHS} = (1 - \alpha_{loss}^{SHS}) S_{w,t-1}^{SHS} + (P_{w,t,abs}^{SHS} \eta_{abs}^{SHS} - P_{w,t,rel}^{SHS} \eta_{rel}^{SHS}) \Delta t, S_{w,t}^{STHS} = 0 \\ 0 \leq P_{w,t,abs}^{SHS} \leq C^{SHS} \\ 0 \leq P_{w,t,rel}^{SHS} \leq C^{SHS} \\ 0 \leq S_{w,t}^{SHS} \leq C^{SHS} \end{cases} \quad (20)$$

Where: $P_{w,t,abs}^{SHS}$ 、 $P_{w,t,rel}^{SHS}$ and $S_{w,t}^{SHS}$ are respectively the hydrogen storage capacity per unit time, hydrogen release capacity per unit time and the total amount of hydrogen remaining in hydrogen storage; η_{abs}^{SHS} 、 η_{rel}^{SHS} and α_{loss}^{SHS} are respectively the hydrogen storage efficiency, hydrogen release efficiency and self-release rate of SHS; C^{SHS} refers to the configured capacity of SHS. SHS is used when STHS can't meet the hydrogen load, and its use order is: real-time hydrogen supplement > STHS > SHS.

Hydrogenation of HFCS should meet certain conditions, and the actual hydrogen amount should not exceed the total capacity of the battery, but at the same time it should not be less than the hydrogen amount expected by users. Suppose that when the shipowner connects HFCS to the hydrogenation pile, the user's own expected information, the desired state of hydrogen charge when hydrogenation leaves is S_h , which means that when the user decides to leave, the actual hydrogen amount of HFCS should be greater than or equal to the expected value, which is expressed as

$$\begin{cases} 0 < S_{st,i} < 1 \\ S_h \leq S_{en,i} \leq 1 \end{cases} \quad (21)$$

Where: $S_{st,i}$ is the hydrogen-loaded state when the i-Th HFCS start hydrogenation, and $S_{en,i}$ is the hydrogen-loaded state when the i-Th HFCS leave.

4. Double-layer optimal dispatching model of ocean island coupled with electricity, hydrogen and transportation

4.1 Upper transportation network-ocean island operation model

Objective function

$$\begin{cases} f_1 = \min(C_{HS} + C_{WT} + C_{PV}) \\ f_2 = \min(\sum_{j=1}^{96} \sum_{i=1}^N x_{ij} p_i p_j \Delta t) \end{cases} \quad (22)$$

Where: f_1 indicates the operating cost of ocean island, where C_{HS} 、 C_{WT} 、 C_{PV} respectively indicate the operating cost of energy storage of hydrogen, wind power generation device and photovoltaic power generation device. f_2 represents the cost of hydrogenation; x_{ij} is the hydrogenation status of the i-Th ship in j period, which have two values: 0 or 1, 0 indicates no hydrogenation, 1 indicates hydrogenation; p_i is the power of the I-Th measuring vessel; p_j represents the price of hydrogen in period j; N represents the number of HFCS ships.

Constraint condition

Constraints of hydrogen energy storage, power balance and HFCS hydrogenation.

4.2 Self-consistent model of lower traffic network-ocean island

Based on the two-way coupling framework of ocean island new energy and transportation network, the

objective function of low-carbon economy optimal dispatching is established, which includes two parts: first, the self-consistency rate of system electric energy and hydrogen energy is the highest; Second, the system has the lowest carbon emission cost.

$$\begin{cases} \eta = \max(\frac{F_{DG}}{F_E} + \frac{F_q}{F_H}) \\ F = \min \alpha C_{CO_2} \\ C_{CO_2} = C_c(E_g - E_c) \end{cases} \quad (23)$$

$$C_c = \begin{cases} -c(1+2\gamma) & E_g < E_c - v \\ -c(1+\gamma) & E_c - v \leq E_g < E_c \\ -c & 0 \leq E_g < E_c \\ c & E_c \leq E_g < E_c + v \\ c(1+\beta) & E_c + v \leq E_g < E_c + 2v \\ c(1+2\beta) & E_c + 2v \leq E_g < E_c + 3v \end{cases} \quad (24)$$

$$E_g = \sum_{t=1}^T (a_1 + b_1 P_t^E + c_1 (P_t^E)^2) \quad (25)$$

$$E_c = \chi \sum_{t=1}^T P_t^E \Delta t \quad (26)$$

Where: η refers to the daily self-consistency rate of ocean-going island coupled with electricity, hydrogen and transportation; F_E refers to the electric load on the island; F_{DG} refers to the output power of DG; F_H is the hydrogen load of transportation network; F_q is the energy supply and output for hydrogen refueling stations; F is the carbon emission cost; α refers to the tax amount for carbon emission, and C_{CO_2} refers to the carbon emission cost. C_c is the carbon transaction price, c is the basic unit carbon price, β is the ladder price increase range, and v is the interval length of carbon emission. γ indicates the reward coefficient in the carbon trading price; E_g is the actual carbon emissions generated from starting the diesel generator, a_1 , b_1 , c_1 is the carbon emission calculation coefficient for diesel generators. E_c is the carbon emission quota for power generation by diesel generators, χ is the carbon emission quota for unit electricity, and P_t^E is the electricity generated by diesel generators in unit time.

Constraint condition

Distribution network operation constraints, electrolytic cell equipment operation constraints, hydrogen fuel cell equipment operation constraints, HFCS and hydrogen refueling stations operation constraints, hydrogen energy storage equipment operation constraints.

5. Model solving

Dung beetle optimization algorithm has fast convergence and strong optimization ability, but it also has some defects such as uneven initial population distribution, unbalanced global exploration and local development ability, easy to fall into local optimization, and may not be able to search the whole solution space effectively, thus unable to get the optimal solution. Therefore, this paper proposes an improved dung beetle optimization algorithm (IDBO).

The DBO algorithm mainly includes four steps.

Step1: Ball rolling behavior

Dung behavior of dung beetles can be divided into obstacle mode and barrier-free mode. When there is no obstacle, the intensity of the light source will affect dung beetle, and the position update during the ball rolling behavior is shown in the following formula 27; When encountering obstacles and unable to move forward, the dancing behavior is simulated by using tangent function, and the position update is shown in the following formula 2.

$$\begin{cases} x_i^{t+1} = x_i^t + \lambda \cdot k \cdot x_i^{t-1} + b \cdot |x_i^t - x_{worst}| \\ x_i^{t+1} = x_i^t + \tan(\theta) |x_i^t - x_i^{t-1}| \end{cases} \quad (27)$$

Where: x_i^t is the position of the eth individual in the t iteration. λ is the random deflection coefficient of [0,1] which is -1 or 1 randomly; b is the random coefficient and x_{worst} is the worst individual position.

Step2: Reproductive behavior

As shown in the following expressions 28, after determining the spawning area, the position of the young ball changes as shown in the following formula 29.

$$\begin{cases} Lb^* = \max \{x_{lbest} \cdot (1 - R), Lb\} \\ Ub^* = \min \{x_{lbest} \cdot (1 + R), Ub\} \end{cases} \quad (28)$$

$$x_i^{t+1} = x_{lbest} + b_1 \times (x_i^t - Lb^*) + b_2 \times (x_i^t - Ub^*) \quad (29)$$

Where: x_{lbest} is the local optimal solution; $R = 1 - \frac{t}{t_{max}}$, t_{max} is the maximum number of iterations, and t is the current number of iterations; Lb is the lower bound and Ub is the upper bound; b_1 and b_2 are two D-dimensional independent random vectors.

Step3: Foraging behavior

Foraging area is simulated by using the boundary selection strategy, as shown in the following formula 30. Foraging dung beetles in a local range, the position update of Xiang beetles is shown in Formula 31.

$$\begin{cases} Lb^* = \max \{x_{gbest} \cdot (1 - R), Lb\} \\ Ub^* = \min \{x_{gbest} \cdot (1 + R), Ub\} \end{cases} \quad (30)$$

$$x_i^{t+1} = x_i^t + C_1 \times (x_i^t - Lb^*) + C_2 \times (x_i^t - Ub^*) \quad (31)$$

Where: x_{gbest} is the global optimal solution, C_1 is the D-dimensional random vector with normal distribution, and C_2 is the D-dimensional random vector with [0,1].

Step4: Stealing behavior

The best food source is the most suitable place to compete for food. The location of stealing oyster mantis is

updated as follows:

$$x_i^{t+1} = x_i^t + S \times g \times (|x_i^t - x_{gbest}| + |x_i^t - x_{lbest}|) \quad (32)$$

Where: s is a constant and g is the D -dimensional random vector that obeys normal distribution.

IDBO algorithm aims at the problem that the distribution ratio of the four kinds of actions of the original dung beetle algorithm is uneven, and each individual can only perform one kind of action, which may lead to insufficient search for the solution space or slow convergence. This paper uses the dung beetle action mutation strategy and reverse learning strategy based on population similarity to improve DBO.

Improvement point one: Strategy of Dungeon Action Variation Based on Population Similarity

In order to make each dung beetle perform four kinds of actions, this paper simulates the time change with the number of iterations, and mutates the dung beetle's actions every m iterations to mutate the current actions into the next behavior strategy. Cosine similarity is used to measure population similarity, and population diversity is expressed as follows:

$$Diver = \frac{1}{N} \sum_{i=1}^N \frac{\sum_{j=1}^d x_{i,j}(t) x_{glbest,j}(t)}{\sqrt{\sum_{j=1}^d x_{i,j}^2(t)} \sqrt{\sum_{j=1}^d x_{glbest,j}^2(t)}} \quad (33)$$

When $Diver$ is greater than 0.5, the population diversity is too low, and it may fall into local optimum. The ability and convergence speed to explore the solution space is determined by the number of ball-rolling dung beetles and foraging dung beetles.

Therefore, individuals who perform breeding and foraging behaviors are mutated into individuals who perform ball rolling behaviors, and the global search ability is enhanced to enhance species diversity, so that new best individuals can be found or the mutated individuals can be restored to the original behavior individuals to continue searching after reaching the iterative threshold T_{max} of the mutated individuals.

Improvement point two: Reverse learning strategy

Because the global search ability of breeding and stealing behavior will decrease with iteration times, and the idea of reverse learning strategy is to select a better solution by generating the reverse solution of the current feasible solution and comparing the fitness of the reverse solution with the original solution, this paper uses reverse learning strategy to improve global search ability of breeding and stealing behavior:

$$x_r^t = lb + ub - rand(\cdot) \times x_i^t \quad (34)$$

$$x_i^t = \begin{cases} x_i^t, & f(x_i^t) < f(x_r^t) \\ x_r^t, & f(x_r^t) < f(x_i^t) \end{cases} \quad (35)$$

Where: x_r^t is the inverse solution; lb and ub are D -dimensional vectors, which represent the lower bound and upper bound of each dimension; $rand(\cdot)$ is the D -dimensional random vector and x_i^t is the current feasible

solution.

To sum up, figure 2 shows the flow of IDBO algorithm.

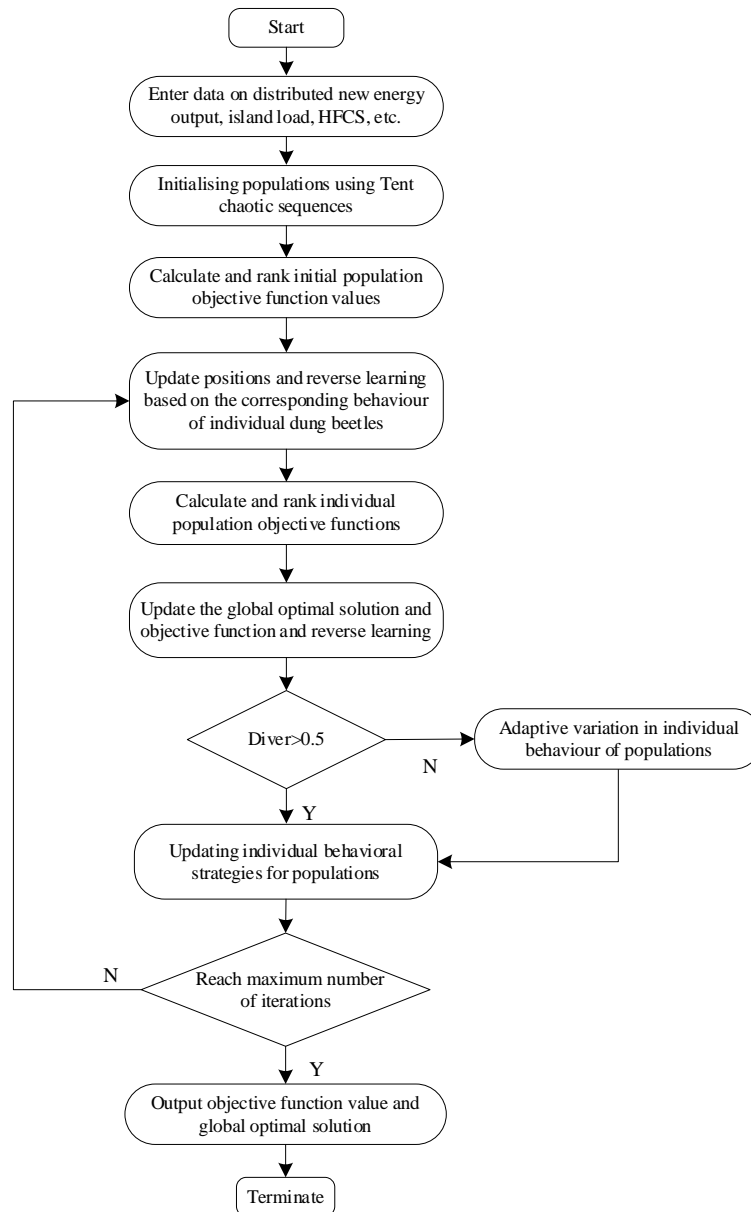


Figure 2. Model solving process based on IDBO

6. Example analysis

This paper takes an island as the research object. In the power grid, the island adopts an improved IEEE standard 6-node grid structure with rated voltage of 10kV, and scaled proportionally. Considering the standby factor of the unit, the island is equipped with a diesel generator with rated power of 400kW, and wind and light represent forms of renewable energies. The island is equipped with a fan with rated power of 180kW and a photovoltaic device with power of 200kW. In the transportation network, a main station and two sub-stations are designed, and the coupling is realized through hydrogen refueling stations. The island adopts an improved IEEE 6-node system as shown in Figure 3.

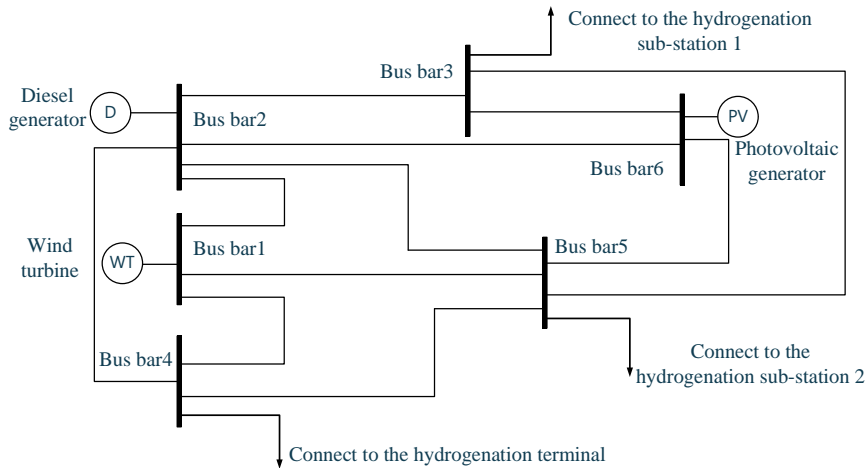
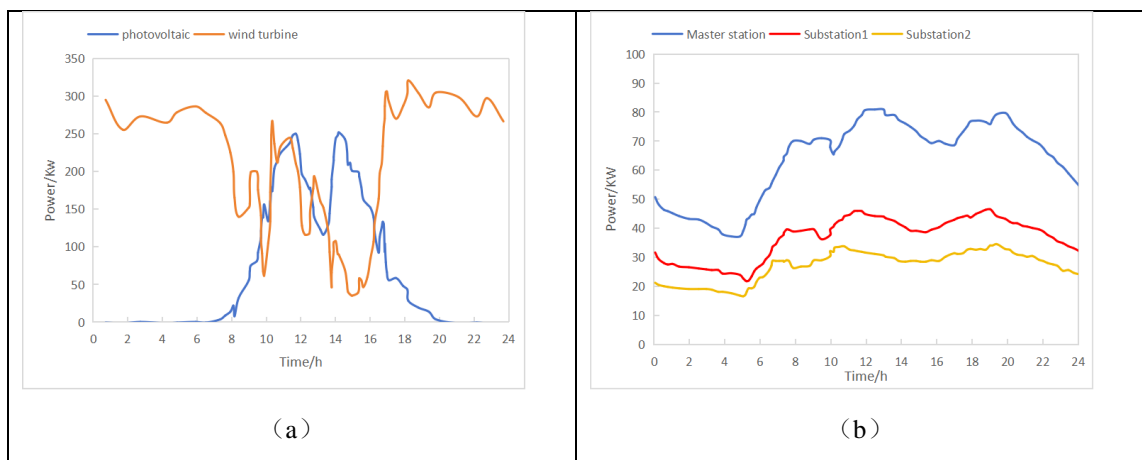


Figure 3. Improved IEEE 6-node system diagram

In the coupling example of electricity-hydrogen-traffic, the main hydrogenation station is equipped with STHS and SHS. There are only STHS in the hydrogenation substation, that is, the hydrogenation substation cannot transport hydrogen energy to the hydrogenation main station, and hydrogen energy can not be mutually assisted between the hydrogenation substations. If the wind-solar distributed energy can't meet the demand of hydrogen load, the STHS of the hydrogenation station will make up for it first. If there is still a shortage of hydrogen energy, the SHS of the hydrogenation station will be called by the transport ship.

The example takes 24 hours a day as the scheduling cycle, the unit scheduling time is 15 minutes, and the scenery is 15 minutes. The output curve of distributed energy of scenery is shown in Figure 4(a), and the electric load curve is shown in Figure 4(b). The hydrogen load curve is shown in Figure 4(c). The maximum number of HFCS per day in the main hydrogenation station is 10, and the maximum number of HFCS per day in the substations 1 and 2 is 6. The real-time hydrogen price in this area is shown in Figure 4(d). The total capacity of hydrogen storage equipment in the main hydrogenation station is 40kg, and the total capacity of hydrogen storage system in the substation is 20kg. The transportation time of the hydrogen energy transshipment ship is 4:00 pm. The diesel generator consumes 1kW·h to produce 0.96kg of CO₂ and 25.2g of hydrogen.



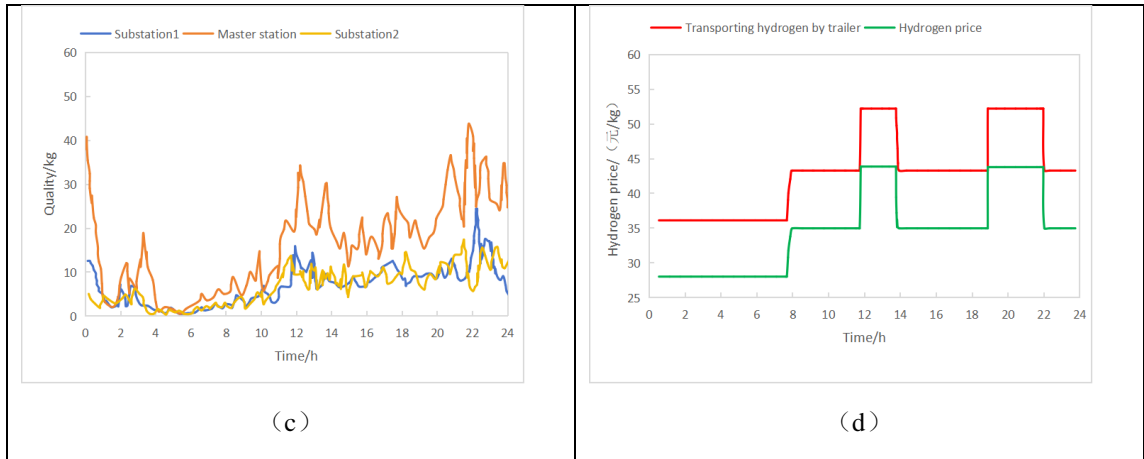


Figure 4. Basic data

Firstly, compare IDBO with DBO algorithm, and the comparison of its main station algorithm is shown in Figure 5.

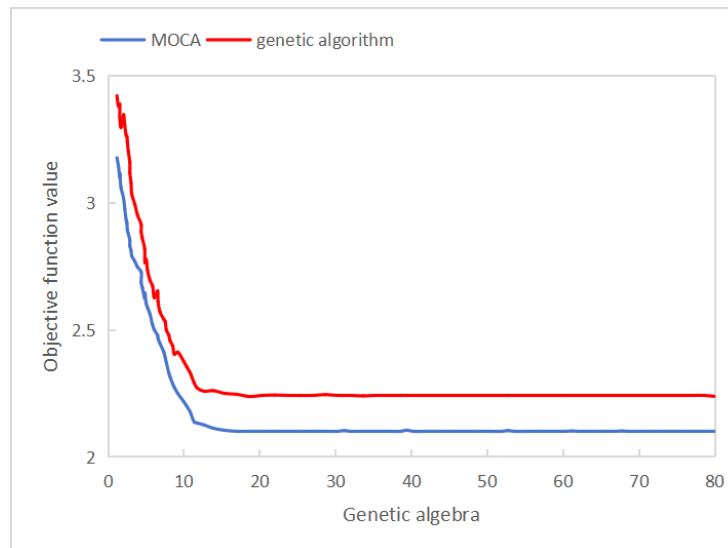


Figure 5. Iteration of Basic Data Algorithm

In Figure 5, compared to the traditional DBO algorithm, IDBO has higher speed and accuracy. Therefore, this paper uses IDBO to optimize the original hydrogenation data. The comparison before and after optimization is shown in Table 1, and the optimized hydrogenation data is shown in Figure 6.

Table 1. Comparison Results of Optimization

Before and after comparison	terminal		Substation 1		Substation 2	
	Peak-valley difference /kg	Hydrogenation cost/yuan	Peak-valley difference /kg	Hydrogenation cost/yuan	Peak-valley difference /kg	Hydrogenation cost/yuan
front	4.968	6124.1	2.85	3157.6	2.18	2896.4
after	4.173	4813.5	1.88	1951.4	1.65	1812.8

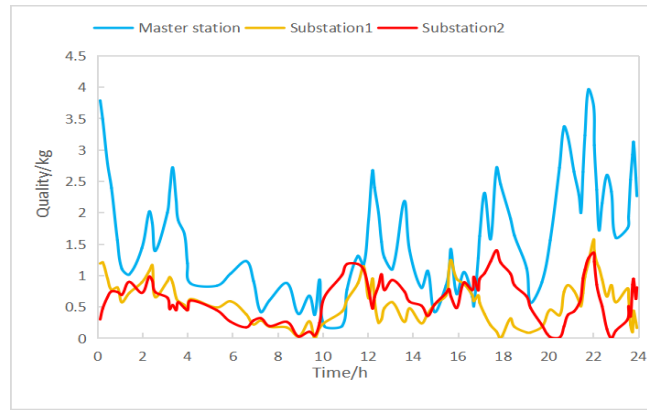


Figure 6. Optimized Hydrogenation Data Map

Compared to this, the price of hydrogenation at the port is reduced by 21.4%, and the peak is reduced by 16.0% in the valley. The hydrogenation rate of port 1 decreased by 38.2% and the difference from peak to valley by 34.0%. The hydrogenation cost of substation 2 decreased by 37.4%, and the peak-valley difference decreased by 32%. It can be seen that the transportation network hydrogenation model can effectively reduce the user's hydrogenation cost and peak-valley difference.

Comparative analysis of schemes

Four schemes are set as an example, and the hydrogen energy saving method of each scheme is shown in Table 2.

Table 2. Hydrogen Energy Storage Scheme

plan	one	two	three	four
STHS	✗	✓	✗	✓
SHS	✗	✗	✓	✓

Note: it means that the situation is not considered, and it means that the situation is considered. ✓ indicates that the situation is taken into account, ✗ is not taken into account.

According to the requirements of the power distribution system, the island's integrated power supply meets the demand of the electrical load, and the degree of electrical power is 100%. We analyze the compatibility level of hydrogen energy from the energy demand of hydrogen load and select the corrected hydrogenation data and the hydrogen production process of the hydrogen base. Table 3 shows the calculation results of the energy balance level and carbon cost of each system.

Table 3. Calculation Results of Hydrogen Energy Storage Scheme

plan	terminal		Substation 1		Substation 2	
	Self-consistency rate%	Carbon emission cost/yuan	Self-consistency rate%	Carbon emission cost/yuan	Self-consistency rate%	Carbon emission cost/yuan
one	78.91	60.45	71.03	31.75	68.55	33.76
two	95.15	5.13	88.23	10.23	91.32	11.98
three	✗	✗	80.13	18.31	79.34	21.03
four	95.15	5.13	98.21	3.13	100	0

Note: ✗ indicates that the situation is not considered.

The analysis results of the example in Table 3 show that:

- 1) In Scheme 2, the energy self-consistency rate of the hydrogen station is increased by 17.06% compared with Scheme 1, and the carbon emission cost is reduced by 91.5%. The calculation results show that STHS can effectively improve the energy self-consistency rate and reduce carbon emissions.
- 2) In Scheme 3, the energy self-consistency rate of hydrogenation substation 1 is increased by 12.81% and the carbon emission cost is reduced by 42.3%, while that of substation 2 is increased by 15.74% and the carbon emission cost is reduced by 37.7%. The calculation results show that SHS can improve the energy self-consistency rate and reduce carbon emission.
- 3) By comparing Scheme 2 and Scheme 3, it can be seen that STHS is better than SHS in the case of single configuration of hydrogen energy storage. Because STHS has the characteristics of local energy utilization and cross-time balance, it meets the needs of local energy consumption and high self-consistency of the system.
- 4) Four schemes are compared and analyzed, among which scheme 4 is the best calculation result. Therefore, the combination of STHS and SHS is the best choice to improve energy self-consistency and reduce carbon emissions. The order of hydrogen energy supply is: hydrogen production from wind and light distributed energy surplus electricity, STHS, SHS, and hydrogen production from diesel generator.

There are STHS and SHS in the hydrogenation terminal in Scheme 4. If the residual hydrogen energy is less than 0.8kg, all of it will be stored in STHS; If the residual hydrogen energy is greater than 0.8kg, 0.8kg is STHS, and the remaining hydrogen energy is shared energy storage, as shown in Figure 7. The operation of the main station and substations 1 and 2 is shown in Figures 8 and 9.

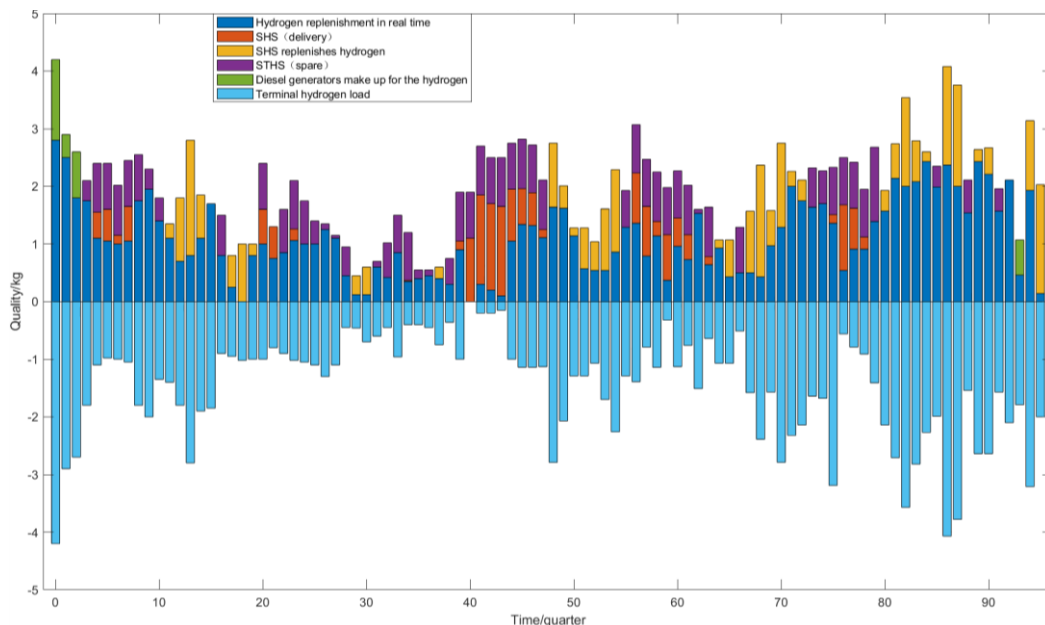


Figure 7. Operation of Scheme 4 Main Station

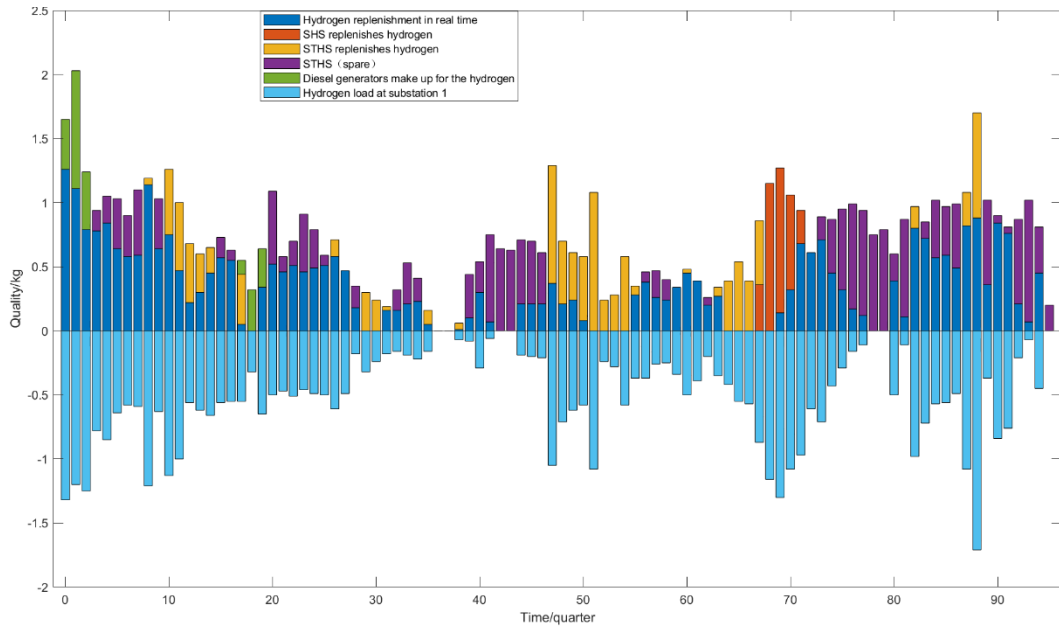


Figure 8. Operation of Substation 1 in Scheme 4

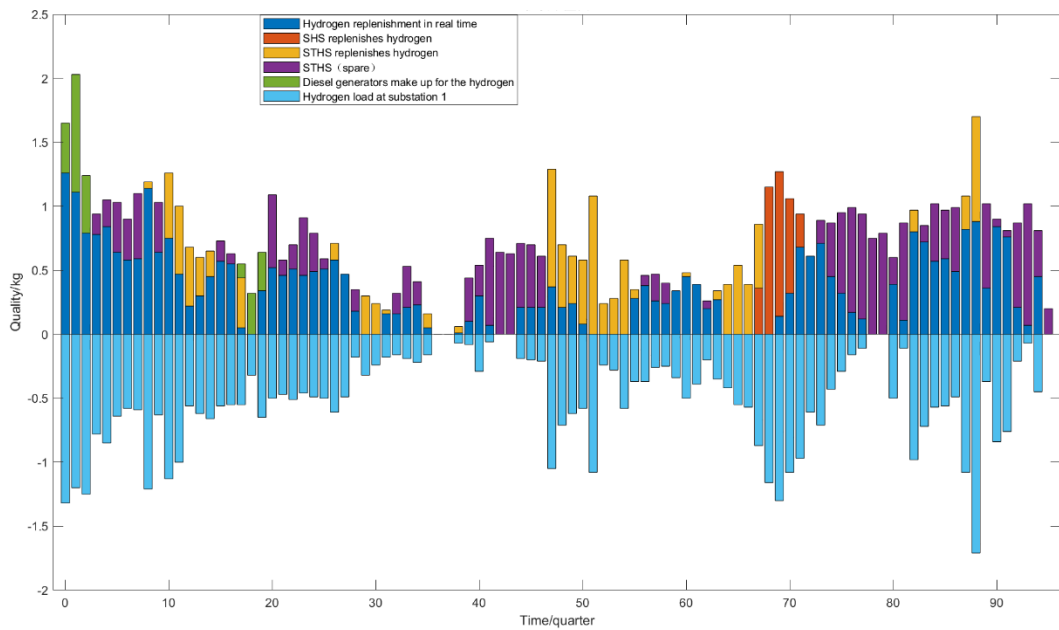


Figure 9. Operation of Substation 2 in Scheme 4

The above optimization results show that:

- 1) In Figure 7, the energy self-consistency rate of Scheme 4 and Scheme 2 is 95.15%, because in both schemes, there are only STHS in the hydrogenation terminal, and it is necessary to rely on diesel generators to generate electricity and produce hydrogen.
- 2) In Figure 8, STHS and SHS jointly support the operation of Hydrogenation Sub-station 1, and the energy self-consistency rate is 97.07%, and 14.28kg of hydrogen is produced by purchasing electricity from the upper power grid, resulting in a carbon emission cost of 3.13 yuan.
- 3) In Figure 9, STHS and SHS jointly support the operation of the hydrogenation substation 2, and the energy

self-consistency rate reaches 100%, so there is no need for diesel generator to generate electricity and no carbon emission cost. It can be seen that improving the self-consistency rate of energy can effectively reduce the cost of carbon emissions.

4) In the early hours of the morning, the wind and scenery distributed energy output is small and the hydrogen reserves are insufficient, so the island needs to rely on diesel generators to generate electricity.

5) After 18: 00, the output of wind and solar distributed energy decreased, but the demand for HFCS hydrogenation increased, which made hydrogen production from surplus electricity unable to meet the demand for hydrogen load. First, it was supplemented by the shared energy storage of hydrogenation substations. The above optimization results show that the self-consistent energy system is of great value to reduce carbon emissions and improve energy self-consistency rate.

6 Conclusion

In this paper, an optimal dispatching model of low-carbon economy for offshore islands considering energy self-consistency rate and SHS is proposed. Building a self-consistent energy system can fully tap new energy and flexible adjustable resources in the maritime transportation network, which is of great value to realize local energy consumption, reduce diesel generator power generation, thus reducing carbon emissions and realizing low-carbon and green. The main conclusions are as follows:

- 1) Under the condition of small wind and solar distributed energy output and insufficient hydrogen reserves, the main reason for increasing the carbon emission cost of the system is that the offshore island relies on diesel generators for power supply;
- 2) The configuration of STHS and SHS on the ocean island coupled with electricity, hydrogen and transportation can improve the energy self-consistency rate and reduce the carbon emission cost;
- 3) When STHS and SHS of hydrogen refueling station cooperate, energy has the characteristics of multi-time and space transfer, with the highest energy self-consistency rate and the lowest carbon emission cost. It can be seen that improving the energy self-consistency rate promotes the energy coordination between systems, reduces the dependence on diesel generators, and is of great significance for reducing carbon emissions.

The research results of this paper can provide useful reference for the low-carbon economic operation of offshore islands and maritime transportation networks under the background of energy transformation.

Author Contributions: Conceptualization, Yibo Liu, Yirui Wang; methodology, Yibo Liu, Qianfei Xu; writing—original draft preparation, Yibo Liu, Yirui Wang, Yuxuan He; supervision, Supeng Wu; software, Qianfei Xu, Yirui Wang.

References

- [1] Chen Y-T, Kuo C-C, Jhan J-Z. Research on Energy Storage Optimization Operation Schedule in an Island System. *Applied Sciences*. 2021; 11(8):3690.
- [2] Żołądek M, Figaj R, Kazantzakis A, et al. Energy-economic assessment of self-sufficient micro grid based on wind turbine, photovoltaic field, wood signifier, battery, and hydrogen energy storage. *International Journal of Hydrogen Energy*. 2024, 52: 728-744.

- [3] Itemize M, Cinder I. Cleaner production of energy and fuels from a renewable energy-based self-sufficient system with energy storage options. *Journal of Energy Storage*. 2023, 72: 108415.
- [4] Hardy S, Er gun H, Van Hemmer D. A greedy algorithm for optimizing offshore wind transmission topological. *IEEE Transactions on Power Systems*. 2021, 37(3): 2113-2121.
- [5] Parasol S, Mutation K M, Suntan D. A novel configuration of a hybrid offshore wind-wave energy conversion system and its controls for a remote area power supply. *IEEE Transactions on Industry Applications*. 2022, 58(6): 7805-7817.
- [6] Huang C Y, Bu T T, Lin W M, et al. Energy Sustainability on an Offshore Island: A Case Study in Taiwan. *Energies*. 2022, 15(6): 2258.
- [7] Lin X, Chen , Zhou X, et al. Integrated Energy Supply System of Pelagic Clustering Islands. *Proceedings of the Chinese Society of Electrical Engineering*. 2017, ,37(01):98-110.
- [8] Anastasia B, Amazon S, Gropius D, et al. Solar power-to-gas application to an island energy system. *Renewable Energy*. 2021, 164: 1005-1016.
- [9] Cal ado G, Castro R. Hydrogen production from offshore wind parks: Current situation and future perspectives. *Applied Sciences*. 2021, 11(12): 5561.
- [10] Wu W, Chou S-C, Viswanathan K. Optimal Dispatching of Smart Hybrid Energy Systems for Addressing a Low-Carbon Community. *Energies*. 2023; 16(9):3698.
- [11] Succetti F, Rosato A, Araneo R, et al. Challenges and Perspectives of Smart Grid Systems in Islands: A Real Case Study. *Energies*. 2023; 16(2):583.
- [12] Ouyang Y, Zhao W, Wang H, et al. A Multiple Time Scales Rolling Coordinative Dispatching Method for an Island Microgrid with High Proportion Tidal Current Energy Access and Demand Response Resources. *Energies*. 2022; 15(19):7292.
- [13] Heistrene L, Azzopardi B, Sant AV, et al. Stochastic Generation Scheduling of Insular Grids with High Penetration of Photovoltaic and Battery Energy Storage Systems: South Andaman Island Case Study. *Energies*. 2022; 15(7):2612.
- [14] Wu C, Sui Q, Lin X, et al. Scheduling of energy management based on battery logistics in pelagic is landed micro grid clusters. *International Journal of Electrical Power & Energy Systems*. 2021, 127: 106573.
- [15] Sui Q, Bhang R, Wu C, et al. Stochastic scheduling of an electric vessel-based energy management system in pelagic clustering islands. *Applied energy*. 2020, 259: 114155.
- [16] Wang Z, Lin X, Li C, et al. A hybrid transmission network in pelagic islands with submarine cables and all-electric vessel based energy transmission routes. *International Journal of Electrical Power & Energy Systems*. 2020, 120: 106005.
- [17] Xia Shiwei, Tian Ye, Wang Zizheng, et al. An energy scheduling method for clustering islands with shared power exchanging vessels. *International Journal of Electrical Power & Energy Systems*. 2023, 152: 109200.
- [18] Abdeltawab H H, Mohamed Y A R I. Mobile energy storage scheduling and operation in active distribution systems. *IEEE Transactions on Industrial Electronics*. 2017, 64(9): 6828-6840.
- [19] Sun Yingyun, Li Zuyi, Mohammad S, et al. Battery-based energy storage transportation for enhancing power system economics and security. *IEEE Transactions on Smart Grid*. 2015, 6(5): 2395-2402.
- [20] Chen Yingying, Zheng Yu, Luo Fengji, et al. Reliability evaluation of distribution systems with mobile energy storage systems. *IET Renewable Power Generation*. 2016, 10(10): 1562-1569.

ABOUT THE AUTHOR



Yibo Liu was born in Yichang, Hubei, China, in 2002. He is currently studying at the College of Electrical Engineering and New Energy at Three China Gorges University, majoring in Electrical Engineering and Automation. He is currently pursuing a bachelor's degree with a research focus on power system optimization and scheduling.

E-mail: liuyibo1_1@163.com



Yirui Wang is currently studying at the The School of international education at North China Electric Power University. She is currently pursuing a bachelor's degree and she majors in Electrical Engineering and Automation.

E-mail: 19030201658@163.com



Qianfei Xu is currently studying at the The School of Electrical and Electronic Engineering at North China Electric Power University. She is currently pursuing a bachelor's degree and she majors in Electrical Engineering and Automation.

E-mail:18853501718@163.com



Yuxuan He was born in Yichang, Hubei, China, in 2003. She is currently studying at the College of Compute at Hubei University of Education. She is currently engaged in the pursuit of a Bachelor's degree, with a focus on Computer Science and Technology.

E-mail: hyx1289243971@163.com



Supeng Wu was born in Lichan, Hubei, China, in 2002. He is currently studying at the College of Electrical Engineering and New Energy at Three China Gorges University. He is currently engaged in the pursuit of a Bachelor's degree, with a focus on Electrical Engineering and Automation.

E-mail: supengwu123@163.com